RESEARCH AND ANALYSIS OF BIONIC GOLDEN CICADA PEANUT DIGGING SHOVEL
/
仿生金蝉花生挖掘铲的研究与分析

Baiqiang ZUO$^{1)}$, Shuqi SHANG$^{1)}$, Xiaoning HE$^{1)}$, Zelong Zhao$^{1)}$, Dongjie LI$^{1)}$, Wei LIU$^{2)}$, Xu LI$^{1)}$,$^{)}$ Dongwei WANG*$^{1)}$
$^{1)}$ Qingdao Agricultural University, College of Mechanical and Electrical Engineering / China;
$^{2)}$ Shandong Yuanquan Mechanical Co / China
Tel: +86-0532-58957391; E-mail: 200701031@qau.edu.cn
DOI: https://doi.org/10.35633/inmateh-68-64

Keywords: *bionic, design, discrete element model, simulation, test*

ABSTRACT

In order to reduce the high resistance problem during peanut digging shovel operation and improve the soil loosening effect, a bionic peanut digging shovel was designed according to the streamlined profile of the head of the golden cicada, and the range of values of the digging operation parameters was analyzed. A discrete element model was developed to verify that the operational resistance of the bionic excavation shovel is lower than that of the flat shovel. The reliability of the simulation test was confirmed by conducting a resistance test on the excavation shovel through a soil trench test. A three-factor, three-water orthogonal combination test was designed to determine the optimal operating parameters of the excavation shovel: the bevel angle of the shovel blade was 55°, the digging depth was 130 mm, and the width of the shovel face was 309 mm. The paper can provide a reference for designing and optimizing peanut-digging shovels.

摘要

为了减少花生挖掘铲作业时阻力大的问题，提高土壤松动效果。根据金蝉头部的流线型轮廓，设计了一种仿生花生挖掘铲，并分析了挖掘作业参数的取值范围。建立离散元模型，验证仿生挖掘铲的作业阻力低于平面铲。通过土槽试验，对挖掘铲进行阻力测试试验，验证仿真试验的可靠性。设计三因素三水正交组合试验，确定挖掘铲的最佳作业参数：铲刃斜角为 55°，挖掘深度为 130mm，铲面宽度为 309mm。该文可为花生挖掘铲的设计与优化提供参考。

INTRODUCTION

The peanut-digging shovel is a critical component of the peanut harvester, and the operational effectiveness of the peanut-digging shovel determines the quality and efficiency of the harvest (*Jiang et al., 2021; Yang et al., 2019*). The magnitude of the resistance during the operation of the excavation device also has an important impact on the power loss (*Zhang et al., 2021*). The design and optimization of peanut digging shovels can reduce the working resistance and soil ability to dig shovels into improving the functional quality of the peanut harvester (*Shi et al., 2015*).

To reduce resistance and consumption, many scholars have conducted relevant research on excavation devices for root crops. Foreign scholars conducted anatomical tests on mole cricket and studied the drag reduction performance of mole cricket body structure and pointed out that mole cricket forefoot was more developed (*Godwin R J, 2007; Mouazen A M et al., 1999)*. Tillmann W et al. applied some bio-non-smooth forms to metal tribology, and through test analysis, the friction and bonding effects of metal surfaces with bio-non-smooth forms were improved *(Tillmann W et al., 2017).* Lang Chong created a Panax ginseng seedling digging shovel based on pangolin claw toes and scales and demonstrated its excellent soil-breaking ability and clay reduction effect using discrete element tests (*Lang et al., 2020*). Li Changming Shen studied and designed a bionic peanut-digging shovel using the forefoot of mole crickets as a bionic prototype and proved its excellent drag reduction effect through tests (*Li et al., 2020*). Wang Yujing et al. used the discrete element method to simulate the excavation of a new bionic excavation shovel. The results showed that the excavation shovel has a higher soil fragmentation rate and a lower excavation resistance (*Wang et al., 2017*). Therefore, the design optimization of agricultural machinery mechanisms through the theory of bionics has an excellent operational effect.

In this paper, from the perspective of bionics, based on the streamlined curve of the head profile of the golden cicada, a mathematical model of the fitted curve is established, and a peanut-digging shovel imitating the head profile curve of the golden cicada is designed.

The working resistance of the bionic excavation shovel was verified to be lower than that of the flat shovel by discrete element test and soil trench test. According to the agronomy of peanut planting, the bionic digging shovel operation parameters were optimized and analyzed.

MATERIALS AND METHODS

Design of bionic digging shovel

Related studies have shown that shovel shapes have different disturbance effects on the soil and the resistance they are subjected to. The concave shovel has the highest resistance, and the convex shovel is slightly better than the flat shovel, but the curvature of the convex shovel is difficult to determine (*Fan, 2020*). Yang Ranbing designed a streamlined excavation shovel, and only theoretical analysis was conducted without testing its practical effects (*Yang, 2009*). Based on the digging ability of the golden cicada, its head profile has a good effect of loosening soil and reducing climbing resistance. A bionic peanut-digging shovel is designed for its streamlined head profile to explore the possibility of its drag reduction further.

Golden Cicada Contour Line Extraction and Fitting

Using a 3D scanner, the information on the outer contour of the golden cicada is collected and processed to obtain a 3D model of the golden cicada.

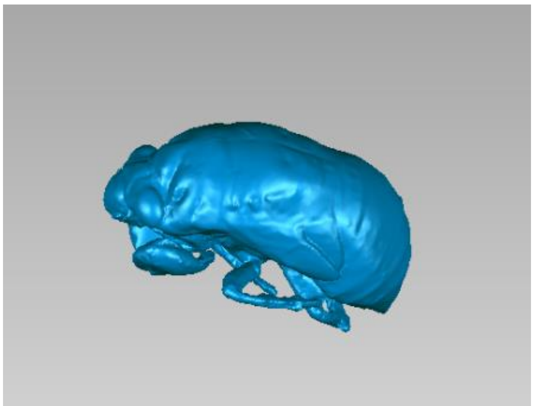

Fig. 1 - Golden Cicada 3D Scanning Model

Import the scanned model of the golden cicada into SolidWorks and use the software to generate a clear and complete profile curve of the head of the cicada. The angle is evenly divided into 12 coordinate points, and the information on the left point is recorded, as in Table 1.

Table 1

Golden Cicada head profile coordinate points

Serial number	1	2	3	4	5	6	7	8	9	10	11	12
x	122.81	132.00	141.72	152.35	164.13	177.20	191.54	206.94	223.07	239.63	256.42	273.34
y	189.10	203.47	217.54	230.89	243.25	254.23	263.47	270.83	276.43	280.60	283.69	286.03

The extracted coordinate points are imported into MATLAB software for processing, and the fitted curves of the coordinate points are obtained. The nth-order polynomial is chosen for fitting the curve equation, and the index of simulation evaluation accuracy can be expressed as the correlation coefficient R^2 of the fitted curve equation.

The equations of the fitted curves are shown in Table 2.

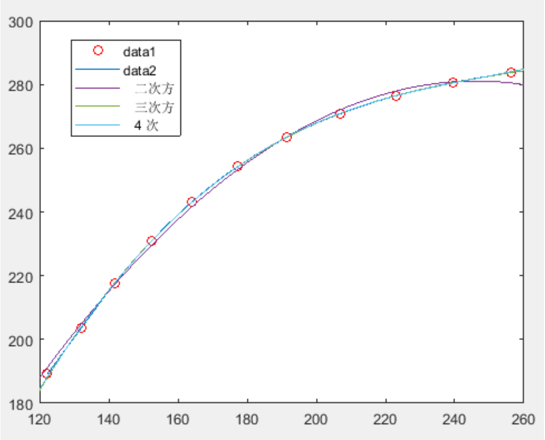

Fig. 2 - Golden cicada head profile fitting curve

Table 2

Curve fitting equation

Fitting the model	Fitting equation	Correlation coefficient R^2
quadratic polynomial	$y=-0.0059*x^2+2.9*x-74$	0.9970
Third order polynomial	$y=2.7e^{-05}*x^3-0.021*x^2+5.7*x-2.4e^2$	0.9999
Fourth order polynomial	$y=6.7e^{-08}*x^4-2.4e^{-05}*x^3-0.007*x^2-1.7e^2$	0.9999

A more considerable R^2 value indicates a higher accuracy of the fitted curve equation. In the case of the same precision, the lower-order equation is preferred to facilitate the subsequent bionic design. The final third-order polynomial was used as the correct equation for the head profile curve of the golden cicada.

Bionic excavation shovel model

Select the spline curve in SolidWorks software and find the equation-driven angle. The obtained fitted equation is imported, and the appropriate scale is adjusted. The bionic digging shovel model is shown in Fig 3.

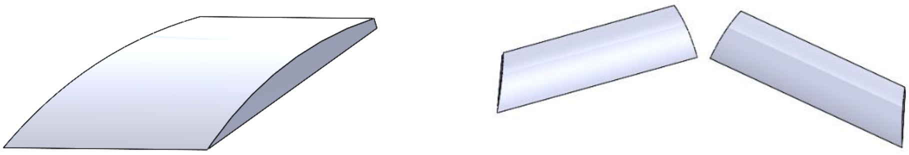

Fig. 3 - Bionic excavation shovel 3D model

Design of working parameters of excavation shovel

Bevel angle of shovel blade

The size of the angle of the shovel blade determines the cutting performance of the excavation shovel on the soil when it enters the ground. To ensure that the environment is cut smoothly and slides away along the edge, improve the self-cleaning ability of the excavation shovel. The bevel angle γ of the shovel surface should satisfy the following:

$$\begin{cases} Q = PQ\cos\gamma \\ T = R\tan\varphi \\ R = P\sin\gamma \end{cases} \tag{1}$$

Conditions for generating slip cuts:

$$Q > T \tag{2}$$

The solution gives:

$$\gamma < 90^{\circ} - \varphi \tag{3}$$

Where:

γ indicates the bevel angle of shovel blade, (°）;

ϕ denotes the angle of friction between the rootstock and the soil on the shovel blade, （°）;

T denotes the frictional force of the rootstock and soil sliding backward, (N).

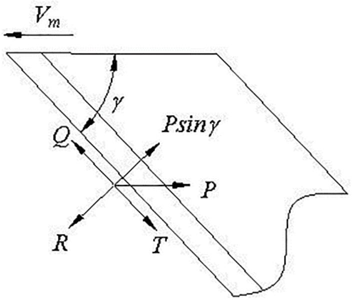

Fig. 4 - Slip-cutting force analysis of shovel blade

The larger the angle of the shovel blade, the larger the digging shovel area, resulting in increased digging resistance; The smaller the digging shovel, the smaller the shovel blade, which is prone to fracture and breakage problems (*Wang et al., 2019*). According to the relevant literature study (Wang et al., 2012), the shovel blade bevel angle range was determined to take the value of 55~65°.

Width of shovel surface

The width of the body of the excavation shovel should be greater than or equal to the width of the distribution of peanut roots in the soil. The width of the shovel body is also related to the planting row spacing, plant spacing, deviations in the forward direction of the digging operation, and irregular deviations of the monopoly. The width of the shovel should be reduced as much as possible on the premise of ensuring the clearance rate of peanut pods to achieve a certain drag reduction effect. The analysis determined that the width of the shovel face is 300~350 mm.

Digging Deeper

Spektor M test studied the nonlinear relationship between the forward resistance and the digging depth in the process of soil cutting by the shovel (*Spektor M., 1981*). The digging resistance becomes continuously more significant with increasing digging depth, ensuring that other parameters remain unchanged (*Chen et al., 2005*). Consider peanut results in a depth of between 80 and 120 mm. It is essential to both reduce the rate of peanut loss and ensure that the digging resistance is as low as possible. Determine the excavation depth of 130~150 mm.

Discrete element model selection

The interaction between the excavation shovel and the soil is a complex movement process. The actual soil trench test could not observe the soil's movement to the excavation shovel. Therefore, the relationship between the action of the excavation shovel and the soil is studied from a macroscopic point of view through discrete element simulation.

Discrete element model selection

The research object of this paper is the soil-excavation shovel system; combined with the actual working condition of the peanut harvester, the contact model is chosen as Hertz-Mindlin with the Bonding model. The model can bond two adjacent soil particles together by a binding force that can withstand tangential and normal displacements.

Soil model construction

In literature (*Chen et al., 2013；Ucgul et al., 2015*), soil particles are set into more than 10 mm spheres. The research shows that the radius of soil particle model is too large, which will affect the calculation accuracy of simulation (*Mark J et al., 2012*). In this paper, in order to control the simulation time in a reasonable range, the soil particle model was developed into spherical particles with a particle size of 3 ~ 5 mm.

As shown in Fig 5, simulated soil tanks with a length of 2000 mm, a width of 800 mm and a height of 400 mm were used to generate soil particles using EDE's particle factory. After all, the particles settle and stabilize, the excavation shovel is imported into EDEM for simulation, and the resistance of the excavation shovel is solved.

Table 3

Basic parameters of discrete element simulation

Parameters	Numerical value
Soil particle density（kg/m³）	1540
Soil Poisson's ratio	0.32
Soil shear modulus (Pa)	$1*10^8$
65Mn density（kg/m³）	7810
65Mn Poisson's ratio	0.29
Elastic modulus of 65Mn (Pa)	$8*10^{10}$
Coefficient of restitution between soil particles	0.56
Coefficient of static friction between soil particles	0.31
Coefficient of dynamic friction between soil particles	0.15
Coefficient of restitution between soil and excavation shovel	0.16
Coefficient of static friction between soil and excavation shovel	0.47
Coefficient of dynamic friction between soil and excavation shovel	0.20

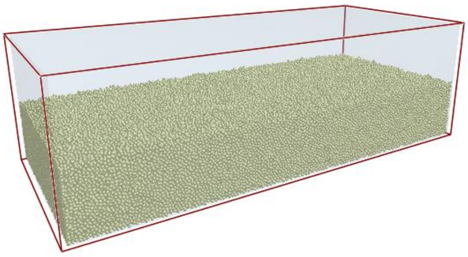

Fig. 5 - Soil model

Simulation test and result analysis

After importing the bionic digging shovel and flat shovel into the model and setting their parameters, start the simulation operation. After the test is completed, the schematic diagram of the simulated motion at three different moments is intercepted. It can be analyzed that there are some differences in the action of the two excavation shovels on the soil during the simulation.

During the operation of the bionic excavation shovel, the speed of the soil does not vary much and tends to be in a steady state. And the velocity of soil particles around the flat excavation shovel increased significantly. The disturbance effect of the bionic digging shovel is better than that of the flat digging shovel.

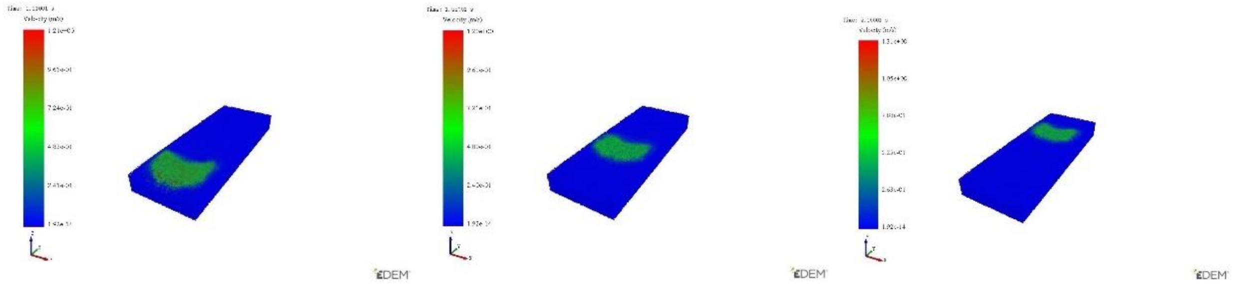

Fig. 6 - Bionic digging shovel

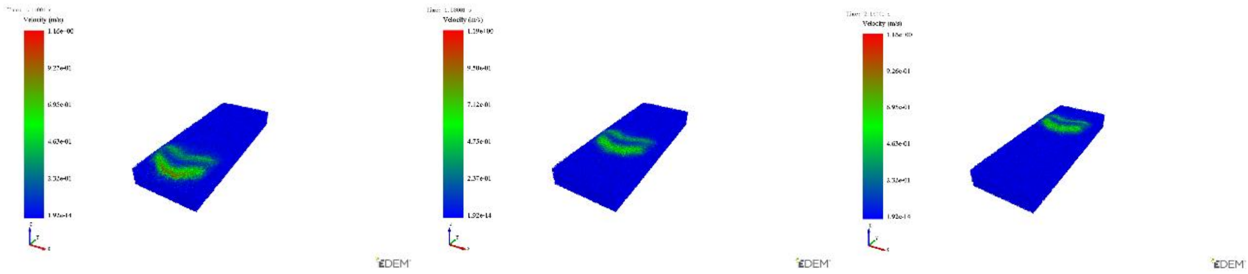

Fig. 7 - Flat excavation shovel

In order to analyze more directly the relationship between the action of the excavation shovel and the soil, the magnitude of the excavation resistance was derived by post-processing, as shown in Fig 8.

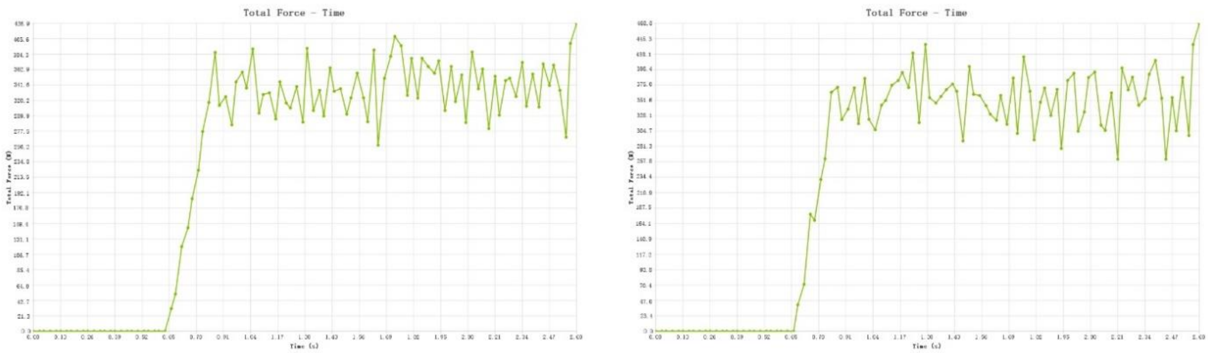

（a）Bionic digging shovel （b）Flat excavation shovel

Fig. 8 - Excavation resistance diagram

According to the digging resistance diagram, it can be analyzed that the bionic digging shovel has a specific resistance reduction ability. The average resistance of the bionic digging shovel was 331.42, and the moderate digging resistance of the flat shovel was 349.73, with a reduced rate of 5.2%. Changing the operating parameters of the excavation shovel and conducting several tests have proven that the bionic excavation lowering ability is better than that of the flat excavation shovel.

Soil Trough Test

Through simulation tests, it was concluded that the bionic excavation shovel has a particular resistance reduction ability. However, the simulation test has some differences from the actual test. Therefore, the soil trough test bed is used to further explore the resistance of bionic excavation shovel and plane shovel. Bionic digging shovel and flat digging shovel size take 1:1 for design. Conduct several tests and take the average value according to the digging resistance change data graph, as shown in Table 4.

Fig. 9 - Soil Tank Test Stand

Table 4

Comparison of soil tank test data

Serial number	Bionic digging shovel	Flat shovel	Resistance reduction rate
1	471.13	515.27	8.6%
2	424.46	476.31	10.9%
3	409.62	454.96	10.%
4	474.17	522.83	9.3%

The resistance reduction rate of the bionic excavation shovel was obtained from the measured resistance difference by the soil trench test. In the actual test, the measured digging resistance value was higher than the simulated test value due to the soil condition and the shovel handles into the soil.

However, the comparison of test data proved the reliability of the simulation test and the resistance reduction effect of the bionic excavation shovel.

RESULTS

Bionic excavation shovel operation parameters optimization test

The drag reduction effect of the bionic digging shovel was verified by simulation and soil trench test. To further determine the optimal combination of parameters for the excavation unit, the shovel blade bevel angle, digging depth, and shovel face width are the test factors, and the digging resistance is selected as the test index. The Box-Behnken test was conducted using the response surface method, and each group of tests was repeated three times to obtain the average value. The test factors and codes are shown in Table 5.

Table 5

Experimental factors and levels

Factor level	—1	0	1
Bevel angle of shovel blade	55	60	65
Digging Deeper	130	140	150
Width of shovel surface	300	325	350

The experimental design scheme and results are shown in Table 6.

Table 6

Test plan and results

Serial number	X1 Bevel angle of shovel blade °	X2 Digging Deeper mm	X3 Width of shovel surface mm	Y1 Excavation resistance %
1	60	140	325	446.61
2	55	150	325	489.41
3	60	150	300	487.82
4	60	140	325	442.37
5	55	140	300	401.27
6	65	130	325	439.26
7	65	140	350	503.76
8	65	150	325	505.92
9	60	140	325	451.42
10	60	140	325	442.37
11	60	130	350	455.79
12	55	130	325	415.37
13	60	150	350	534.62
14	60	140	325	439.62
15	55	140	350	460.62
16	65	140	300	427.86
17	60	130	300	414.36

Analysis of test results

The data were analyzed for ANOVA using Design-Expert 13 software; the results are shown in Table 7. The regression equation between the excavation resistance and the three factors is also established.

Table 7

Analysis of variance for mining resistance

Sources	Squares	DF	MS	F value
Model 1	20817.06	9	33.32	< 0.0001
X_1	1516.08	1	21.84	0.0023
X_2	10730.39	1	154.58	< 0.0001
X_3	6242.91	1	89.94	< 0.0001
X_1X_2	13.62	1	0.1962	0.6712
X_1X_3	68.48	1	0.9865	0.3537
X_2X_3	7.21	1	0.1039	0.7567
X_1^2	48.07	1	0.6926	0.4328
X_2^2	1926.63	1	27.76	0.0012
X_3^2	223.06	1	3.21	0.1161
Residual	485.91	7		
Lack of Fit	400.68	3	6.27	0.0542
Pure Error	85.22	4	R2	0.9772
Cor Total	21302.96	16	Adj R2	0.9479

Note: highly significant (P<0.01); significant (P<0.05).

P-values for the excavation resistance model were less than 0.001, with highly significant differences; the F and P values of the corresponding misfit terms were 6.27 and 0.0542, respectively, which were both greater than 0.05, and there was no significant difference in the misfit terms. The quadratic regression equation fitted by the model is consistent with the actual one and can predict the test results better.

Response surface plots were established to visually analyze the relationship between the influences of the three factors on the test indexes, as shown in Fig 10.

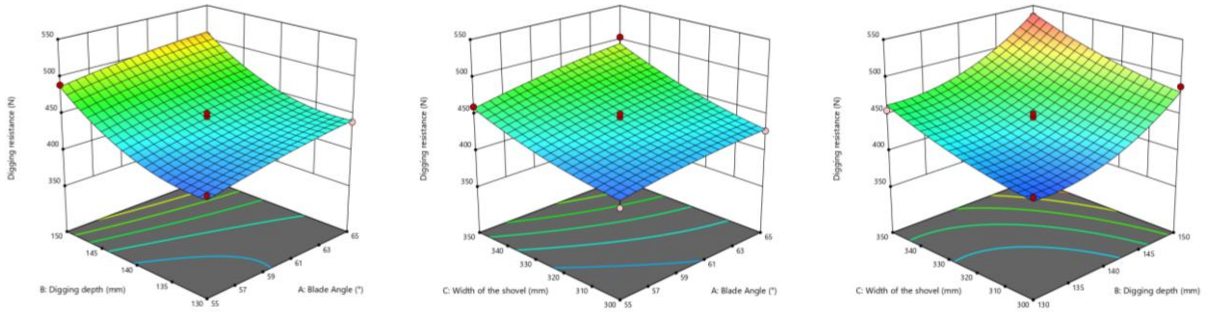

(a) (b) (c)

Fig. 10 - Response surface of the effect of factor interactions on excavation resistance

From figure 10(a), it can be analyzed that the digging resistance increases with the increase of the shovel face inclination. The digging depth is 130~138 mm, the digging resistance rises slowly, and after exceeding 138 mm, the resistance increases sharply. Figure 10(b) can be analyzed: the digging resistance increases with shovel face width and blade inclination angle. Still, the digging resistance is more obviously affected by the shovel face width factor. Figure 10(c) shows that the increase in shovel face width and digging depth cause a sharp rise in resistance. Comprehensive analysis shows that the inclination angle of the shovel blade will lead to a slight increase in the shovel surface area but has little influence on the resistance; the drag resistance is significantly affected by the rise of the excavation shovel surface and excavation depth. Therefore, the effect of the three on the digging resistance needs to be considered comprehensively to reduce the digging resistance as much as possible.

Optimized design of excavation unit

The optimization solution module of Design Expert data analysis software is used to optimally solve the regression equation model for one of the established indicators. The optimum working parameters of the excavation device are: the bevel angle of the shovel blade is 55°, the excavation depth is 130 mm, and the width of the shovel surface is 309 mm. And the excavation resistance is 399.29 N at this time.

To verify the accuracy of the predictions of the described model, soil trench tests were carried out for analysis using the above optimal combination of working parameters, and the results are shown in Table 8.

Table 8

Analysis of test results

Projects	Test average (N)	Model optimization value (N)	Relative Error (%)
Excavation resistance	407.54	399.29	2.0

Due to the influence of the uncertainty of the test, resulting in a relative error of 2%, the bionic excavation shovel operating parameters are reasonably designed.

CONCLUSIONS

(1) The mathematical fitting model was obtained after processing by extracting the coordinates points of the golden cicada's head profile. And a bionic peanut-digging shovel was designed according to the fitted equation.

(2) The discrete element model is established, and the simulation test concludes that the drag reduction effect of the bionic excavation shovel is better than that of the flat excavation shovel. Soil tank tests further verified the reliability of the simulation results.

(3) Three factors and three levels of tests were designed to determine the optimal working parameters of the excavation shovel: the bevel angle of the shovel blade is 55°, the digging depth is 130 mm, and the width of the shovel face is 309 mm. This study may provide a reference for the optimal design of peanut digging shovel.

ACKNOWLEDGEMENT

This research was funded by Modern Agricultural Industrial Technology System Project (CARS-13) and Shandong Provincial Key Science and Technology Innovation Engineering Project (2021CXGC010813).

REFERENCES

[1] Chen Y, Lars J M, Tavs N. (2013). A discrete element model for soil-sweep interaction in three different soils [J]. *Soil & Tillage Research*, 126: 34－41.

[2] Chen Zhihua, Li Yaoming, Sun Xingzhao. (2005). Dynamic analysis and experiment of peanut excavating shovel（花生挖掘铲动力学分析与试验）, *Transactions of the Society for Agricultural Machinery,* Vol.36, Issue 11, pp. 59-63.

[3] Fan Yu. (2020). *Research on potato digging mechanism and design of biomimetic shovel based on discrete element method (基于离散元法的马铃薯挖掘机理研究及仿生铲设计).* Master dissertation, Shenyang Agricultural University. China National Knowledge Internet.

[4] Godwin R J. (2007). A review of the effect of implement geometry on soil failure and implement forces [J] *Soil and Tillage Research,* 97 (2):331-340.

[5] Jiang Yanjin, Chen Lidong, Li Guofang et al, (2021). Research progress of peanut harvester excavating device（花生收获机挖掘装置的研究进展）, *Journal of Hebei Normal University of Science and Technology*, Vol.35, Issue 4, pp. 59-63.

[6] Lang Chongchong, Xu Lulu, Pan Wujian et al. (2020), Design and finite element analysis of bionic excavating shovel for Panax Notoginseng seedlings（三七种苗仿生挖掘铲设计与有限元分析）, *Chinese Journal of Agricultural Mechanization,* Vol.41, Issue 9, pp. 88-94

[7] Li Changming. (2020). *Design and analysis of bionic mole cricket groundnut digging shovel*（仿生蝼蛄花生挖掘铲的设计与分析）, Master dissertation, Shenyang Agricultural University, *China National Knowledge Internet.*

[8] Mark J., Chen Y., Sadek M.A. (2012). Determining parameters of a discrete element model for soil-tool interaction [J]. *Soil & Tillage Research*, 118:117-122.

[9] Mouazen A M, Nemenyi M. (1999) Tillage tool design by the finite element method: Part 1. Finite element modelling of soil plastic behavior [J]. *Journal of Agricultural Engineering Research,* 72（1):37-51.

[10] Shi Chao, Yang Ranbing, Shang Shuqi. (2015). Finite element statics analysis of peanut harvester excavating device based on UG. （基于 UG 的花生收获机挖掘装置有限元静力学分析）, *Agricultural mechanization research,* Vol.37, Issue 1, pp. 18-21

[11] Spektor M. (1981), Principles of soil-tool interaction [J]. *Journal of Terramechanics,* 18(1):51-65.

[12] Tillmann W., Stangier D, Lopes-Dias N.F. et al. (2017). Adjustment of friction by duplex-treated, bionic structures for Sheet-Bulk Metal Forming [J]. *Tribology International,* 111: 9-17.

[13] Ucgul M., John M.F., Chris S. (2015). Three dimensional discrete element modeling (DEM) of tillage: accounting for soil cohesion and adhesion [J]. *Biosystems Engineering*, 129: 298－306.

[14] Wang Fangyan, Sun Guangquan, Shang Shuqi. (2019). Development of 4CL-1 self-propelled combined harvest machine for green onion (4CL-1 型自走式大葱联合收获机的研制), *Transactions of the CSAE,* Vol.35, Issue 24, pp. 39-47

[15] Wang Jiasheng, Shangshu Banner. (2012). Development and experiment of self-propelled double row combined carrot harvester (自走式双行胡萝卜联合收获机的研制及试验), *Transactions of the CSAE,* Vol.28, Issue 12, pp. 38-43

[16] Wang Yujing, Wang Yicai, Liu Ziwen et al. (2017). Simulation analysis of new bionic excavating shovel based on discrete element method（基于离散元法的新型仿生挖掘铲的仿真分析）, *Chinese Journal of Agricultural Mechanization,* Vol.38, Issue 3, pp. 23-26

[17] Yang Li, Dai Kejie, Zhang Tong et al, (2019). Design and optimization of excavating shovel for peanut harvest（花生收获挖掘铲设计及优化）. *Agricultural engineering*, Vol.9, Issue 7, pp. 80-83.

[18] Yang Ranbing. (2009). *Design and Experimental study on Main equipment of HQL-2 peanut Combined Harvester (HQL-2 型花生联合收获机主要装置的设计与试验研究)*. Master dissertation, Shenyang Agricultural University. *China National Knowledge Internet.*

[19] Zhang Hailiang, Zhao Fengqin. (2012). Static analysis of excavating shovel based on ANSYS（基于 ANSYS 的挖掘铲静力分析）, *Agricultural technology and equipment*, Vol.5, pp. 13-15.